Synthesis of Fe(II)/Co(II)-Fused Triphenyl Porphyrin Dimer as Candidate for Oxygen Reduction Reaction Catalyst

Atmanto Heru Wibowo[1*], Anggit Pradifta[1], Abu Masykur[1], Ken-ichi Yamashita[2], Yosuke Tani[2], Ari Yustisia Akbar[2], and Takuji Ogawa[2]

[1]*Research Group of Synthesis and Material Functionalization, Department of Chemistry, Universitas Sebelas Maret,*
Jl. Ir. Sutami 36A, Surakarta, Indonesia

[2]*Department of Chemistry, Graduate School of Science, Osaka University, Machikaneyama-cho 1-1,*
Toyonaka-city, Osaka, 560-0043, Japan

** **Corresponding author:***

tel: +62-85878677541
email: aheruwibowo@staff.uns.ac.id

Received: November 26, 2020
Accepted: April 20, 2021

DOI: 10.22146/ijc.61671

Abstract: *This paper reports the synthesis of Fe(II)/Co(II) fused triphenyl porphyrin dimers as candidate of hybrid organic metal electrocatalyst. The synthesis was conducted in five-step reactions using the starting materials pyrrole and benzaldehyde. The fuse oxidative reaction was done via free-base form of triphenyl porphyrin to omit metal insertions/removals of intermediate products. This strategy is very beneficial for the synthesis of metal fused triphenyl porphyrin that needs less reactions where phenyliodine(III) bis(trifluoroacetate) (PIFA) was successfully deployed in the oxidative reaction of two free-base triphenyl porphyrins. Here, the comparisons of NMR spectra were presented to see the changes of the starting material to the product. Initial electrochemical tests showed that reduction current of planar structure of Fe/Co fused triphenyl porphyrin dimer was on the potential range at -1.10 V to 0.45 V vs Au. Fe-fused triphenyl porphyrin dimer with 7.58 × 10^{-4} A (-1.05 V) showed slightly better performance than Co-fused triphenyl porphyrin dimer with 5.67 × 10^{-4} A (-0.97 V).*

Keywords: *fused triphenyl porphyrin; metal insertion; oxidative reaction; planar structure*

■ INTRODUCTION

In recent years, synthesis of porphyrin compounds has been developed in various fields focusing mostly on determining organic methods for new structures and gaining the benefit of its functionalization of these materials. Porphyrin consists of four methine carbons and four pyrroles with 18π aromatic macrocycle. Until now, synthesis and structure modification of porphyrin macromolecules have been performed to extend its π system in some way from simple to complicated reactions to gain the benefits of electronic system properties in specific applications. Altering the π system in the molecule porphyrin is done by the addition of substituent groups owing also π system through connection of *meso* and β position carbon atom on main porphyrin structure. Therefore, hundreds of new porphyrin molecules with π system extension and a longer conjugation system than the original porphyrin have been reported up to now. However, extended porphyrins with planar structure of macromolecules have gained more attentions than the non-planar ones due to their effectiveness in the extension of the electronic π system of molecules. Fused porphyrins are of interest in developing new planar structures because of their unique physical properties derived from the narrow HOMO-LUMO gap and supramolecular assemblies based on the intermolecular π-π stacking interaction facilitated by the expanded and planar π conjugation [1]. Therefore, fused porphyrins and metal complexes thereof have attracted considerable interest recently as functional materials for sensor devices, catalysts including photocatalysts and electrocatalysts, nanowires, solar cells, photodynamic therapy, etc., including investigation on magnetic properties [2-3], absorption spectroscopy [4-12], electrochemistry [3,7-8,10-11,13-14], conductivity [15-17] and photovoltaics [18].

In the year 2000, Osuka and coworkers [19] have reported oxidative transformation of *meso-meso* linked diphorphyrins into triply linked fused porphyrins owing a planar-structure form. Since then, reports on fuse synthesis from porphyrin monomer to porphyrin dimers and porphyrin arrays via *meso-meso* or/and β-β connections have been increasingly published. Ouyang et al. [14] has synthesized symmetrically fused triply porphyrin using oxidant of phenyliodine(III) bis(trifluoroacetate) (PIFA) directly on the position of β-β and *meso-meso* of carbon atoms. Fused asymmetrically porphyrin has also been then synthesized by Ryan et al. [20] with triply C–C connections to fused porphyrins bearing different substituents on each porphyrin monomer. This strategy was done by firstly singly fuse synthesis of *meso* position of C atoms via Suzuki coupling of porphyrin priors to oxidation of each 2β positions of two porphyrins. Up to now, various synthesis of fused porphyrins to extend π electron conjugation by porphyrin dimerization [10,21-23] have been reported. Besides, the presence of supporting materials or in combination with bulky functional groups such as triphenylene and polycyclic aromatic hydrocarbons (PAHs) on porphyrins has been synthesized.

In this study, the synthesis of a fused porphyrin dimers with 2D planar structure of two triphenyl porphyrin is performed. The electrochemical properties of this dimer porphyrin for oxygen reduction are also investigated. Fused porphyrin dimers were synthesized with the procedure modification by Ouyang et al. [14], Lee et al. [24] and Ryan et al. [20] where a fair amount of PIFA is used as an oxidation agent. Fuse synthesis is done without the presence of zinc metal in the porphyrin cavity to cut the procedures that are commonly done in the form of zinc porphyrin complex as its intermediate product. The planar structure of Fe(II)/Co(II) porphyrin dimer synthesized with more rigid form is supposed to support the effectivity for oxygen reduction reaction.

■ EXPERIMENTAL SECTION

Materials

All reagents and solvents used were of high purity grade. Pyrrole and pyridine were from Sigma-Aldrich Chemicals. Benzaldehyde, toluene, chloroform, methanol, sodium borohydride ($NaBH_4$), catalyst of trifluoroacetic acid (TFA) and trichloroacetic acid (TCA), trimethyl orthoformate, ferro chloride tetrahydrate ($FeCl_2·4H_2O$), cobalt(II) chloride hexahydrate ($CoCl_2·6H_2O$), dimethylformamide (DMF), sodium carbonate (Na_2CO_3), dichloromethane (CH_2Cl_2), silica gel 60 (230–400 mesh) were all from Merck. Phenyllithium solution was from Tokyo Chemical Industries (TCI), Japan. Phenyliodine(III) bis(trifluoroacetate) (PIFA) and 2,3-dichloro-5,6-dicyano-1,4-benzoquinone (DDQ) were from Shanghai Industries. Silica gel used for the separation was from Merck. All solvents were purchased from Sigma-Aldrich without any further purification.

Instrumentation

^1H and ^{13}C-NMR spectra were taken from AGILENT VNMR 400 Hz instrument. Infrared spectra (IR) were obtained from Shimadzu model Prestige 21. MALDI-TOF was from Kratos PCAxima CFR V2.3.5. Cyclic Voltammetry was from Metrohm μ Autolab type III.

Procedure

Synthesis of 5-phenyl dipyrromethane/PDP (2)

PDP was synthesized based on the report from Lee and Lindsay [25]. Necessary modification was made to fit the apparatus in our laboratory. 150 mL Pyrrole (**1**) (2.16 × 10^3 mmol) and benzaldehyde (6 mL, 59 mmol) were put into a 250 mL three neck flask equipped with magnetic-stirrer bar and connected with nitrogen-gas pipe. The flask was flown with nitrogen for 15 min prior to the addition of TFA (0.45 mL, 5.80 mmol). Stirring of the mixture was done for 15 min at room temperature. The crude product yielded from the reaction was checked with silica TLC with an eluent of DCM:*n*-hexane (70:30) at Rf = 0.82, whereas the pyrrole and unidentified product were checked at Rf = 0.55 and Rf = 0.88, respectively. After the reaction was accomplished, the excess pyrrole was removed with a vacuum rotary evaporator at 60 °C until a viscous brownish black liquid was obtained. Purification of DPP was done by column chromatography with silica (50 g, 230–400 mesh) and eluted with gradient method (DCM:*n*-hexane 60:40, 70:30, 80:20, and DCM). Solvent was then collected and evaporated with vacuum until white crystals of the product were obtained.

Synthesis of 5,15-diphenylporphyrin/DPP (3)

DPP was synthesized and modified as reported by Baldwin et al. [26]. PDP (**2**) (0.5 g, 2.30 mmol) was put in 300 mL DCM in a 500 mL flask and added to trimethyl orthoformate (18 mL, 1.65×10^2 mmol). The flask was covered with aluminum foil to protect from the sun light before the stirring was started. Trichloroacetic acid/TCA (8.83 g, 54 mmol) in 55 mL DCM was added little by little, followed by a 4 h reaction with stirring. Pyridine (15.6 mL) was then added into the mixture. Stirring at room temperature for 17 h was continued. The crude product was controlled using silica TLC with eluent of DCM:*n*-hexane (70:30) at Rf =0.90 (DPP product) and at Rf = 0.82 (PDP). The reaction was stopped after no PDP spot on TLC was seen. The aluminum foil was then discovered and the mixture was exposed to the air for 10 min followed by stirring underneath the sun light and in contact with air for 4 h. Solvent was evaporated in vacuum at 30 °C and the rest of the solid form was put in the vacuum desiccator for 17 h. The purification was done on a column using silica gel and eluent DCM:*n*-hexane (70:30). The eluate was removed with a vacuum evaporator until the purple solid was obtained. Recrystallization was performed using toluene and pyridine.

Synthesis of 5,10,15-triphenylporphyrin/TPP (4)

About 0.1 g (1 equivalent) of DPP (**3**) was put in a 100 mL flask and dissolved in THF. Before in use, the flask was vacuumed and flown with nitrogen for 15 min. Some preliminary synthesizes have been done to investigate the duration time of the reaction at 0 °C. In this study, the lower initial temperature was taken up to -25 °C to avoid too fast oxidation using self-designed cooler. After the temperature was set to -25 °C, phenyllithium (0.16 mL, 6 equivalent) was added slowly into the solution. The temperature was increased up to room temperature prior to stirring for 2 h. Crude product was monitored with silica TLC using eluent DCM:*n*-hexane (70:30) until only one product at Rf=0.93 as the target product was seen and the starting material at Rf = 0.90 disappeared. Quenching was performed with water and THF (1:4, v/v). The solution was then oxidized with 2,3-dichloro-5,6-dicyano-1,4-benzoquinone 1.04 mL (DDQ) (3 equivalent, in 10 mL DCM) for about 30 min. The solvent was removed with a vacuum rotary evaporator. Purification was done with column chromatography using silica gel and DCM eluent. The solvent was then removed with a vacuum evaporator until a light purple solid was obtained. Recrystallization was done with chloroform and methanol.

Synthesis of fused 5,10,15-triphenylporphyrin dimer/FP (5)

Synthesis of the fused porphyrin dimers was done through the reaction of oxidative coupling with 2.5 equivalents of phenyliodine(III) bis(trifluoroacetate) (PIFA). This procedure is modified from the previously reported from [14] and Lee et al. [24], where no zinc metal or metal center was involved in the reaction. About 0.03 g (1 equivalent) TPP (**4**) was dissolved in 50 mL DCM at -25 °C with self-designed cooler. Phenyliodine(III) bis(trifluoroacetate) (PIFA) (2.5 eq) was then added into the solution. The mixture was stirred while the temperature was slowly increased until room temperature. The crude product was identified on silica TLC using DCM:*n*-hexane (70:30) until only one spot of FP product (Rf = 0.98) and no other spots seen. The reaction was quenched with the addition of $NaBH_4$ and CH_3OH. Purification was done with column chromatography using silica gel and DCM eluent. After removal of the solvent, a dark purple solid of FP was obtained.

Insertion of Fe(II) and Co(II) into fused porphyrin dimer (FP)

Synthesis of Fe(II) and Co(II) FP was done by insertion of Fe(II) and Co(II) into the free-base FP (**5**).

Firstly, FP was dissolved in 70 mL DMF. To the solution, $FeCl_2 \cdot 4H_2O$ (1.5 equivalent) was added at room temperature and refluxed for about 1 h. This reaction was controlled with TLC until no FP spot was seen on the plate. The reaction was stopped at the time where only spot was detected (Rf = 0.97). The solution was then added to 80 mL HCl solution (6 M). The precipitate was then filtered and washed with a little amount of 3 M HCl and dried. Similar procedure was also applied for the insertion on free-base FP with $CoCl_2 \cdot 6H_2O$.

Oxygen reduction test with voltammetry cyclic

Fe(II)-FP was dissolved in 50 mL DMF. The solution was then added to 1 M H_2SO_4. Bubbling with N_2 for 2 h was done to remove O_2 dissolved in the solvent. After no dissolved O_2 into the solution, the solution was bubbled with O_2 for 5 min. A certain volume of the solution (15 mL) was tested using cyclic voltammetry at room temperature with scan rate 100 mV/s, voltage range from -5 to 5 volt with a reference electrode of gold (Au). Similar procedure was applied also to the measurement of Co(II) FP.

■ RESULTS AND DISCUSSION

In the general procedure, the critical stage of the reaction was in the third and fourth stage of the reaction, where the fit and controlled condition were required. Therefore, a cooler equipped with an automatic cooler and thermostat up to -25 °C was made to stabilize the temperature during the oxidation reaction with phenyllithium (stage **iii**) and PIFA (stage **iv**). The synthesis method was modified from Lee et al. [24] where the metal center of zinc in the fuse dimer reaction was used. The role of zinc metal was to help in withdrawing electron on the *meso* carbon in the oxidation reaction. This method is beneficial to the *meso-meso* linking of two porphyrins. However, this zinc insertion was not preferred in this fuse reaction, where the target products are Fe/Co-FP. In the common procedure, zinc should be inserted and then removed if the Fe or Co ion would be inserted. This caused inefficiency and time consuming for the whole reactions. To compensate the absence of zinc, careful reaction is

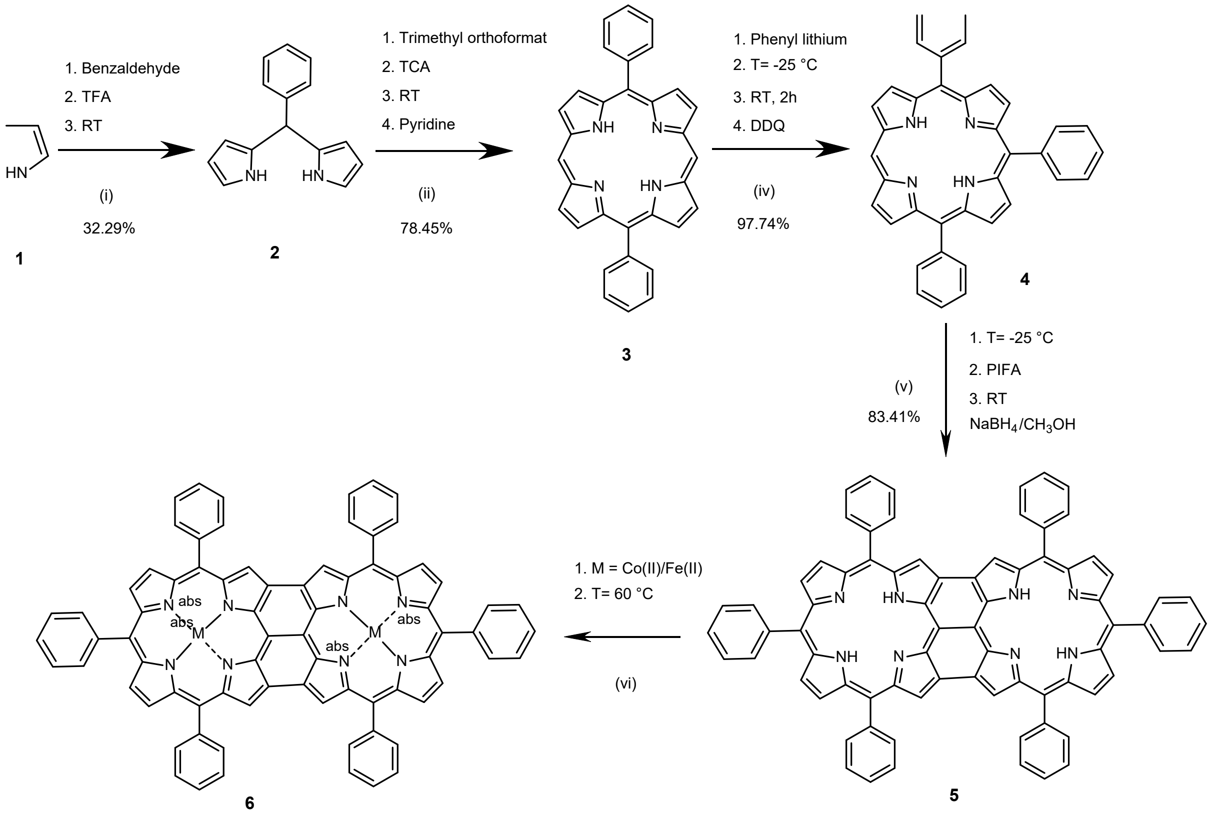

Fig 1. Reaction scheme of the general synthesis of fused triphenyl porphyrin dimer

is done by controlling the temperature with thermostat and to keep the temperature stable in the oxidation reaction. In the dimerization, the initial temperature of the cooler was also adjusted only at -25 °C instead of -75 °C. Ouyang et al. reported that the amount of PIFA added into the fuse reaction influenced the yield of the product. Addition of 2.5 eq PIFA produced the highest yields of only triply linked porphyrins, but increasing the amount of PIFA (up to 5 eq) could depress the dimer yield. Besides, the use of $NaBH_4$ and CH_3OH was also reported well for quenching the oxidation reaction. The following result is of synthesis from the PDP to the target product of Fe/Co-FP. Some NMR spectra comparisons are presented to convince the reaction products.

Synthesis of 5-Phenyl Dipyrromethane/PDP (2)

After purification, PDP product obtained was in the form of white solid about 0.860 g (32.92%), melting point = 101 °C. ^{1}H-NMR spectra of PDP in $CDCl_3$ showed that 7 proton-environment peaks of PDP was found with δH = 7.91 ppm (s, 2H), δH = 7.20–7.33 ppm (m, 5H), δH = 6.68 ppm (d, *J* = 2.4 Hz, 2H), δH = 6.15 ppm (t, 2H), δH = 5.91 ppm (s, 2H), and δH = 5.46 ppm (s, 2H). ^{13}C-NMR spectra in $CDCl_3$ showed that 9 carbons have been identified. Carbons on PDP were identified at δC = 107.18, 108.36, 117.19, 117.23, 126.96, 128.37, 128.63, 132.46 and 142.02 ppm. The yield of the synthesis of PDP was 0.860 g (32.92%)

Synthesis of 5,15-Diphenylporphyrin/DPP (3)

The DPP obtained was about 0.851 g (78.45%) in the form of purple crystal solid, melting point = 302 °C. ^{1}H-NMR spectra of DPP in $CDCl_3$ showed proton groups identified at δH = 10.31 ppm (s, 2H), δH = 9.38 ppm (d, *J* = 2.2 Hz, 4H), δH = 9.08 ppm (d, *J* = 3.4 Hz, 4H), δH = 8.26 ppm (d, *J* = 3.2 Hz, 4H), δH = 7.80–7.36 ppm (m, 6H), and δH = -3.04 ppm (s, 2H). ^{13}C-NMR spectra in $CDCl_3$ showed carbon atom groups at δC = 105.23, 119.10, 126.94, 127.63, 131.02, 131.57, 134.83, 141.37, 145.01, 147.21 ppm. *m/z* = 462.2. The yield of the synthesis of DPP was 0.851 g (78.45%)

The change of NMR spectra from PDP to DPP proved that the reaction of the conversion occurred. The spectra comparison was shown in Fig. 2.

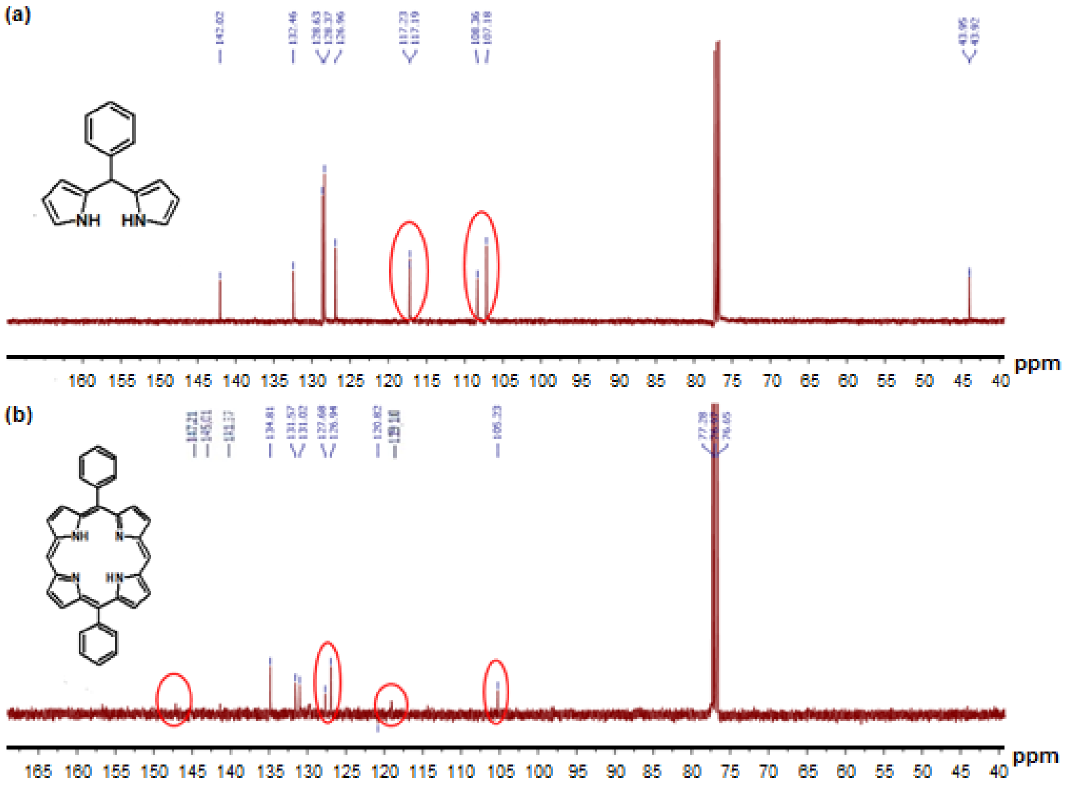

Fig 2. ^{13}C-NMR spectra comparison of (a) 5-phenyl dipyrromethane/PDP and (b) 5,15-diphenyl porphyrin (DPP)

From the Fig. 2, it was clear that the peak number and chemical shift of carbon groups on PDP different from DPP. The carbon groups of pyrrole ring on the PDP was at δ = 106.23, 119.10, 126.94, and 127.63 ppm, whereas DPP showed chemical shift at δ = 107.18, 108.36 and 117.19 ppm. It proved that the condensation of two PDPs with porphyrin was successfully.

Synthesis of 5,10,15-Triphenylporphyrin/TPP (4)

The formation of TPP was an important stage before the fuse reaction. The preliminary investigation of the factors that determine the occurrence of the reaction with phenyllithium has been done. Fig. 3 shows the progress of the reaction of DPP with phenyllithium in different reaction times. From Fig. 3, it was seen that the time reaction was not the main factor in obtaining the TPP product. The mass spectra showed that the 2 h, 14 h, and 17 h reaction times had almost similar mass intensity at *m/z* = 461/462. At initial temperature 0 °C, it was seen that the side products at about *m/z* = 551 appeared. For the further reaction, the lower temperature at -25 °C was chosen to more carefully handle the initial reaction.

The addition of phenyl to DPP with the present of phenyllithium has been successfully carried out with 0.13 g (97.74%) reddish purple powder product (melting point at 295 °C). ^{1}H-NMR spectra of TPP in $CDCl_3$ showed 7 proton groups at δH = -3.04 ppm (s, 2H), 7.76–7.79 ppm (m, 9H), 8.20–8.26 ppm (m, 6H), 8.85–8.90 (d to d, *J* = 13.1–4.8 Hz, 4H,), 9.01–9.02 (d, *J* = 4.4 Hz, 2H), 9.33–9.34 (d, *J* = 4.3 Hz, 2H), 10.21 (s, 1H). ^{13}C-NMR spectra of TPP in $CDCl_3$ showed that 15 carbon atom groups were detected at δC = 104.89, 119.74, 120.67, 126.64, 126.91, 127.48, 127.80, 130.82, 131.57, 134.59, 134.78, 140.46, 140.75, 141.86, 142.65 and 169.36 ppm.

The conversion of the synthesis from the starting material (DPP) into the product of TPP can be proved by the ^{1}H-NMR and ^{13}C-NMR spectra in comparison with DPP and TPP as given in Fig. 4 and 5.

Based on Fig. 5, comparison of ^{1}H-NMR spectra of DPP and TPP showed that new peaks (multiplets) of TPP were seen at δH = 7.77 and 8.23 ppm indicating that one phenyl group from phenyllithium was attached on the DPP. Fig. 5 showed that there were chemical-shifting changes of DPP at 131.02, 131.57, 134.83, and 141.37 ppm to 134.59, 134.78, 140.46 and 140.75 ppm, and carbon of *meso* position on DPP from 147.21 ppm to 169.16 ppm. The yield of the synthesis of TPP was 0.130 g (97.74%).

Synthesis of Fused 5,10,15-Triphenylporphyrin Dimer/FP (5)

The FP after purification was a dark purple crystal about 0.083 g (83.41%) with melting point of 398 °C.

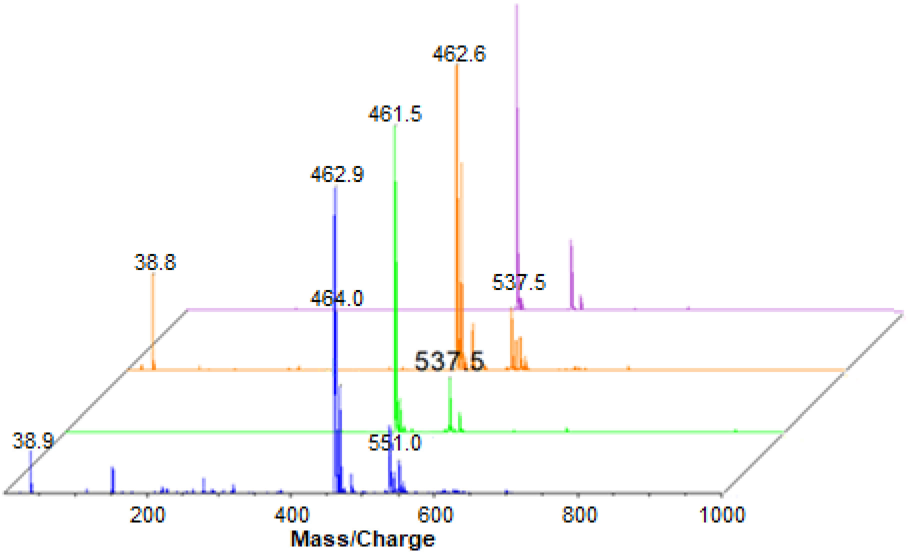

Fig 3. Comparison of mass spectra from MALDI-TOF of the reaction of DPP (1.6 mmol in THF) with phenyllithium after 2 h (blue line), 14 h (green line), 17 h (orange line) reaction and 17 h quenched (purple line) at initial addition temperature 0 °C

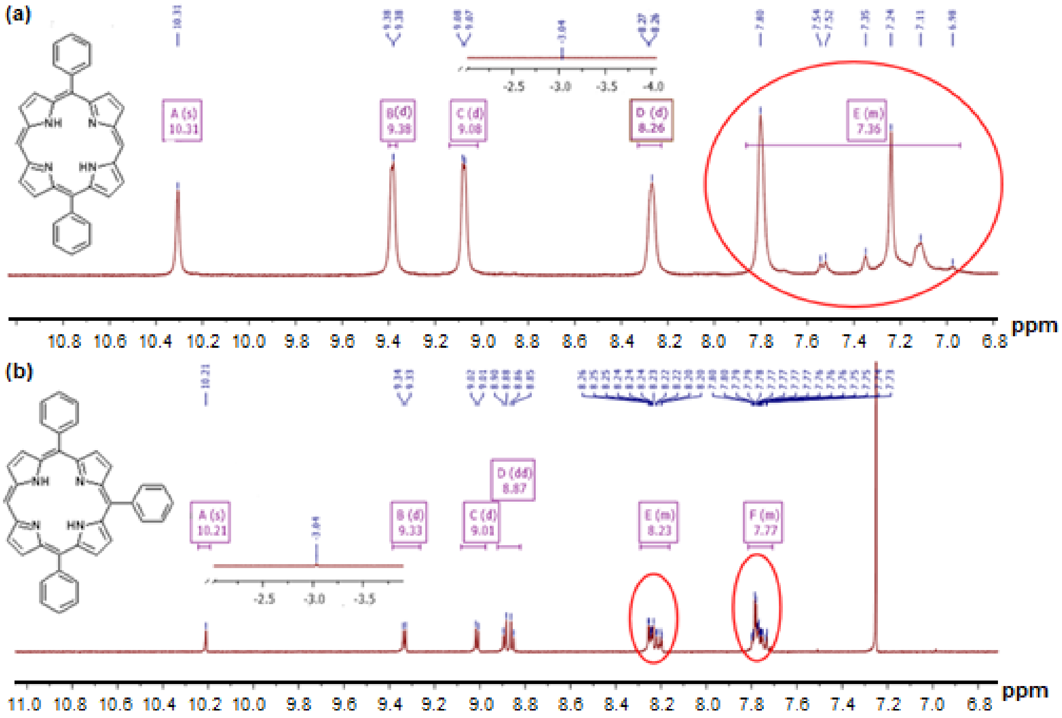

Fig 4. Comparison of ^{1}H-NMR spectra (a) 5,15-diphenylporphyrin/DPP and (b) 5,10,15-triphenylporphyrin/TPP

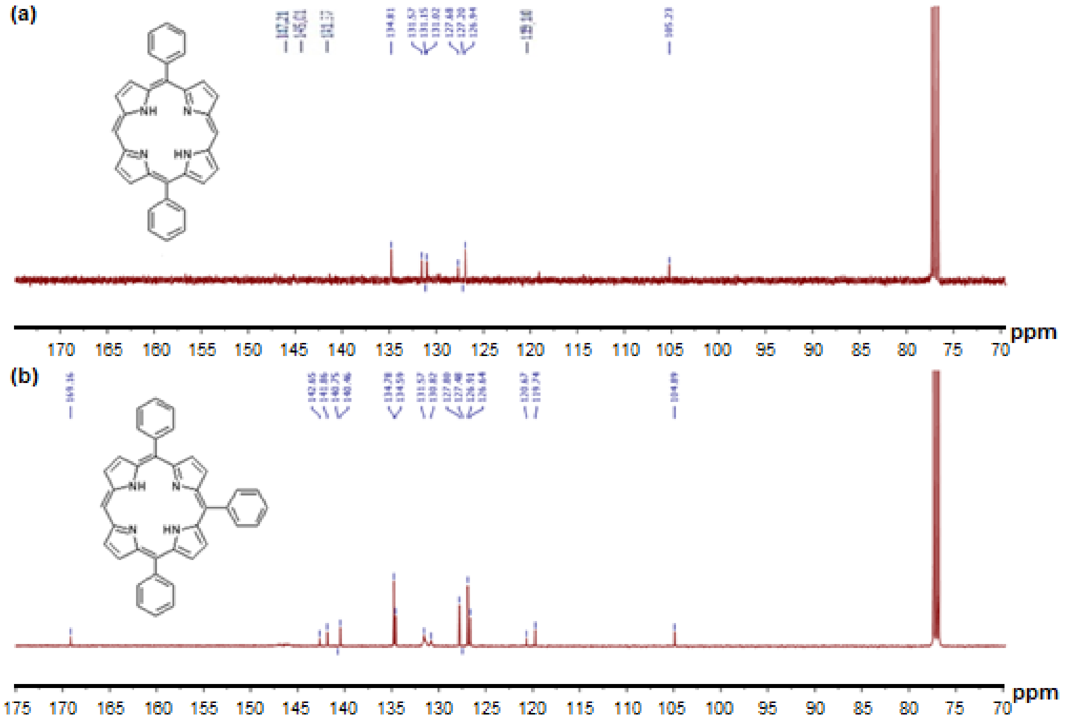

Fig 5. Comparison of ^{13}C-NMR spectra (a) 5,15-diphenylporphyrin/DPP and (b) 5,10,15-triphenylporphyrin/TPP

^{1}H-NMR spectra of FP in $CDCl_3$ showed 6 proton groups with δH = -2.77 ppm (s, 4H), 7.73–7.79 ppm (m, 18H), 8.16–8.21 ppm (m, 12H), 8.77–8.79 ppm (d to d, J = 4.7–3.4 Hz, 4H), 8.90–8.88 ppm (d to d, J = 4.6–3.3 Hz, 4H), 9.63 ppm (s, 4H). Meanwhile, ^{13}C-NMR spectra of FP in $CDCl_3$ showed 23 carbon atoms at δC = 120.73, 120.81, 120.85, 126.64, 126.83, 126.91, 127.54, 127.97, 128.89, 130.96, 131.12, 134.06, 134.53, 134.63, 134.78, 140.77, 141.65, 141.80, 141.99, 169.67, 169.51, 169.36 and *m/z* = 1070.8. The comparison of the spectra of the starting material and the product was done to validate that the reaction was accomplished, as in Fig. 6 and 7.

From the spectra in Fig. 6 and 7, it was seen that there were changes of ^{1}H-NMR and ^{13}C-NMR spectra after reaction. C–H *meso* on the TPP at δ = 10.21 ppm disappeared in the FP spectra. This was caused by the C–H binding to the *meso* position of the two TPPs to form a dimer structure. ^{1}H-NMR spectra of TPP showed a peak (doublet) at δ = 9.33 ppm, whereas the spectra of FP showed a singlet peak at δ = 9.63 ppm. This indicated the change of C–H on the pyrrole ring in TPP. ^{13}C-NMR spectra showed that TPP has peak pattern differences with

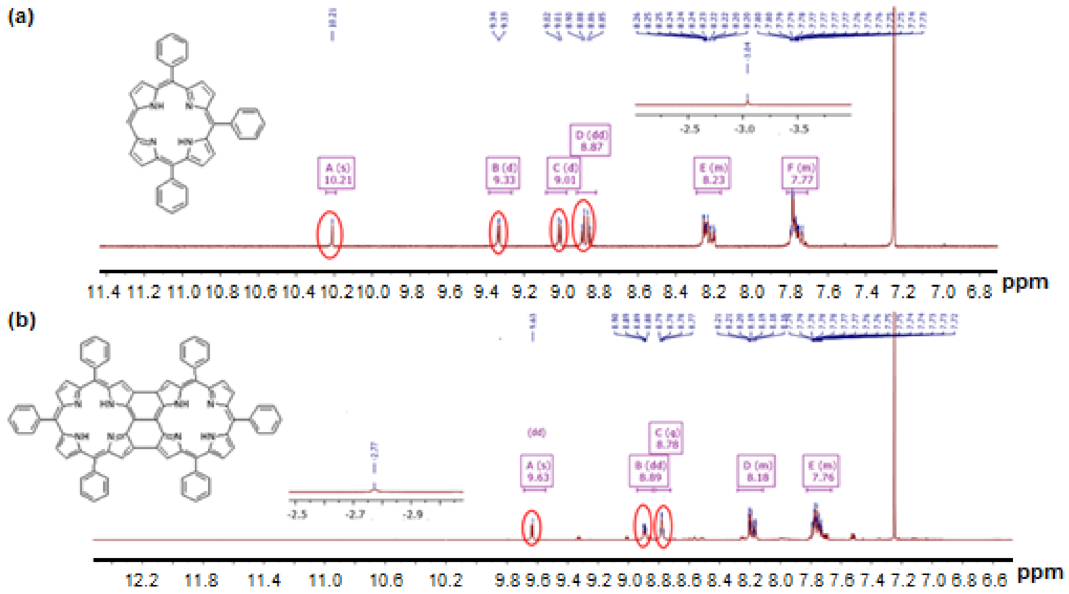

Fig 6. Comparison of ^{1}H-NMR spectra of (a) TPP and (b) FP

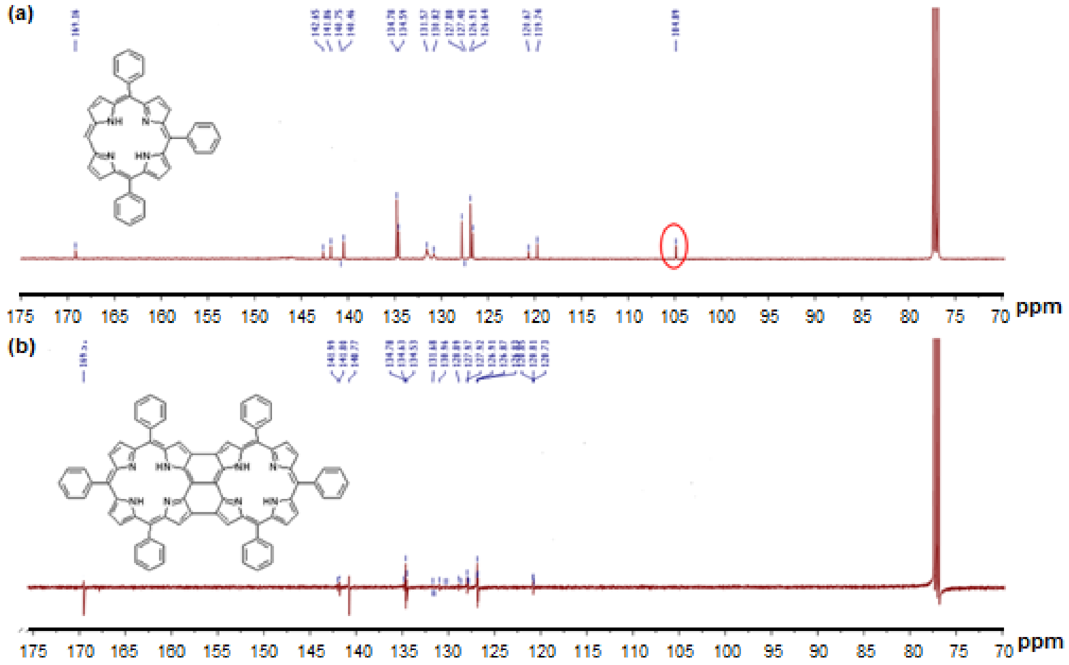

Fig 7. Comparison of ^{13}C-NMR spectra of (a) TPP and (b) FP

FP. A peak at δ = 104.89 ppm was not found on FP spectra, indicating that a dimerization process has already accomplished. The yield of the synthesis of FP was 0.083 g (83.41%)

Insertion of FP with Iron(II) and Cobalt(II) (6)

As the conversion was accomplished, the FTIR data was done to ensure the binding of the N atom to Fe(II) or Co(II) in the cavity of the dimer as seen in Fig. 8.

The metal binding into the porphyrin cavity could be proved from the FTIR spectra (Fig. 8). The absorption peak at about 400–560 cm^{-1} was not found in the FP. Meanwhile, Fe-FP and Co-FP showed absorption peak at 431.11 and 426.29 cm^{-1}, respectively. These absorption peaks indicated that the Fe and Co ions were bonded with the N-atoms in the porphyrin cavities.

Catalytic Test of Fe/Co-FP for Reduction of Oxygen

The result test of Fe/Co FP planar structure (as seen in Fig. 9) using cyclic voltammetry (CV) with voltage scan from -4 to 4 Volt, scan rate = 100 mV/s, T = 25 °C, 1 mm^2 surface area of working electrode and M-FP concentration in DMF = 5 mM was seen in Fig. 10. Voltammogram in the Fe-FP and Co-FP electrodes showed that the reduction current was on the potential range at -1.10 V to 0.45 V vs Au. Reduction potential peak occurred at -1.05 V vs Au. As comparison that the oxygen reduction potential of Pt electrode was reported at 0.40 V vs RHE [27] and the oxygen reduction potential of MOF at 0.60–0.80 V vs RHE [28]. This potential value proved that Fe-FP and Co-FP owe the catalytic activity for oxygen reduction reaction.

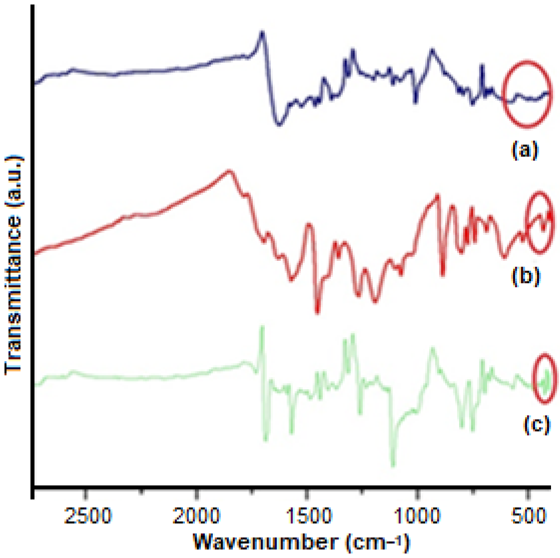

Fig 8. FTIR spectra of FP (a), Co-FP (b) and Fe-FP (c)

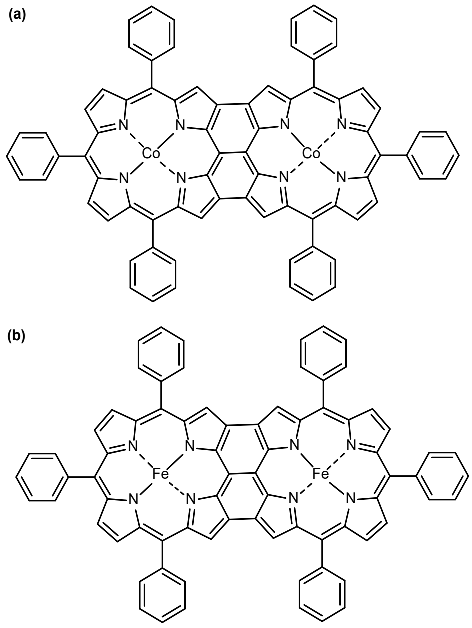

Fig 9. The structure of Co-FP (a) and Fe-FP (b)

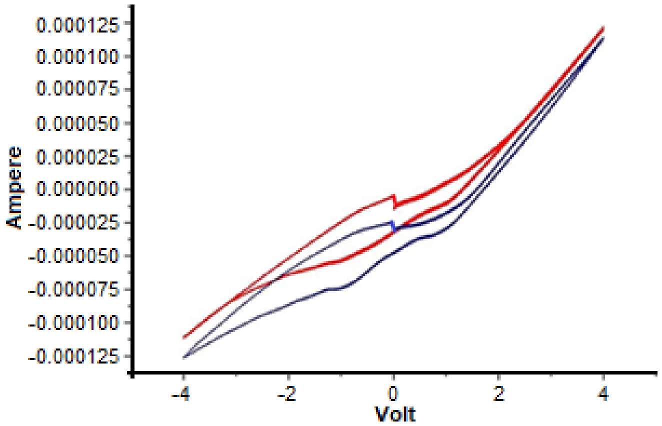

Fig 10. Voltammogram from the Fe FDP (—) and Co-FDP (—) in 1 M H$_2$SO4, saturated with oxygen and scan rate 100 mV/s

Table 1. Peak current and voltage of CV from Fe/Co FDP in DMF with H$_2$SO$_4$ 1 M, saturated with oxygen and scan rate 100 mV/s.

M-FDP	Peak current (A)	Voltage (V)
Fe-FDP	7.58×10^{-4}	-1.05
Co-FDP	5.67×10^{-4}	-0.97

■ CONCLUSION

Synthesis of fused triphenyl porphyrin dimer (FP) could be done without the metal presence (zinc) in the porphyrin cavity or via free-base porphyrin oxidation of *meso* and β carbon of the porphyrin using PIFA. Initial electrochemical tests showed that the planar/coplanar structure of Fe/Co-FP dimers was capable to be employed as a catalyst for oxygen reduction, where Fe-FP showed slightly better performance than Co-FP.

■ REFERENCES

[1] Saegusa, Y., Ishizuka, T., Komamura, K., Shimizu, S., Kotani, H., Kobayashi, N., and Kojima, T., 2015, Ring-fused porphyrins: extension of π-conjugation significantly affects the aromaticity and optical properties of the porphyrin π-systems and the Lewis acidity of the central metal ions, *Phys. Chem. Chem. Phys.*, 17 (22), 15001–15011.

[2] Stähler, C., Shimizu, D., Yoshida, K., Furukawa, K., Herges, R., and Osuka, A., 2017, Stable Ni^{II} porphyrin *meso*-oxy radical with a quartet ground state, *Chem. Eur. J.*, 23 (30), 7217–7220.

[3] Fukui, N., Cha, W., Shimizu, D., Oh, J., Furukawa, K., Yorimitsu, H., Kim, D., and Osuka, A., 2017, Highly planar diarylamine-fused porphyrins and their remarkably stable radical cations, *Chem. Sci.*, 8 (1), 189–199.

[4] Fujimoto, K., Oh, J., Yorimitsu, H., Kim, D., and Osuka, A., 2016, Directly diphenylborane-fused porphyrins, *Angew. Chem. Int. Ed.*, 55 (9), 3196–3199.

[5] Fujimoto, K., and Osuka, A., 2018, A 1,5-naphthyridine-fused porphyrin dimer: Intense NIR absorption and facile redox interconversion with its reduced congener, *Chem. Eur. J.*, 24 (25), 6530–6533.

[6] Fujimoto, K., Shimizu, D., Mori, T., Li, Y., Zhou, M., Song, J., and Osuka, A., 2019, Selective formation of helical tetrapyrrin-fused porphyrins by oxidation of β-to-β linked *meso*-aminoporphyrin dimers, *Chem. Eur. J.*, 25 (7), 1711–1715.

[7] Fukui, N., Cha, W.Y., Lee, S., Tokuji, S., Kim, D., Yorimitsu, H., and Osuka, A., 2013, Oxidative fusion reactions of *meso*-(diarylamino)porphyrins, *Angew. Chem.*, 125 (37), 9910–9914.

[8] Fukui, N., Lee, S.K., Kato, K., Shimizu, D., Tanaka, T., Lee, S., Yorimitsu, H., Kim, D., and Osuka, A., 2016, Regioselective phenylene-fusion reactions of Ni(II)-porphyrins controlled by an electron-withdrawing *meso*-substituent, *Chem. Sci.*, 7 (7), 4059–4066.

[9] Banala, S., Fokong, S., Brand, C., Andreou, C., Kräutler, B., Rueping, M., and Kiessling, F., 2017, Quinone-fused porphyrins as contrast agents for photoacoustic imaging, *Chem. Sci.*, 8 (9), 6176–6181.

[10] Brennan, B.J., Arero, J., Liddell, P.A., Moore, T.A., Moore, A.L., and Gust, D., 2013, Selective oxidative synthesis of *meso*-beta fused porphyrin dimers, *J. Porphyrins Phthalocyanines*, 17 (4), 247–251.

[11] Chaudhri, N., Cong, L., Bulbul, A.S., Grover, N., Osterloh, W.R., Fang, Y., Sankar, M., and Kadish, K.M., 2020, Structural, photophysical, and electrochemical properties of doubly fused porphyrins and related fused chlorins, *Inorg. Chem.*, 59 (2), 1481–1495.

[12] Zhang, P., Yu, C., Yin, Y., Droste, J., Klabunde, S., Hansen, M.R., and Mai, Y., 2020, Bis-anthracene fused porphyrin as an efficient photocatalyst: Facile synthesis and visible-light-driven oxidative coupling of amines, *Chem. Eur. J.*, 26 (69) 16497–16503.

[13] Ishizuka, T., Komamura, K., Saegusa, Y., Tanaka, S., Shiota, Y., Yoshizawa, K., and Kojima, T., 2019, Iron complex of a quadruply fused porphyrin: Synthesis, structure and redox properties, *J. Porphyrins Phthalocyanines*, 24 (01n03), 252–258.

[14] Ouyang, Q., Zhu, Y.Z., Zhang, C.H., Yan, K.Q., Li, Y.C., and Zheng, J.Y., 2009, An efficient PIFA-mediated synthesis of fused diporphyrin and triply–singly interlacedly linked porphyrin array, *Org. Lett.*, 11 (22), 5266–5269.

[15] Baba, K., Bengasi, G., El Assad, D., Grysan, P., Lentzen, E., Heinze, K., Frache, G., and Boscher, N.D., 2019, Conductive directly fused poly(porphyrin) coatings by oxidative chemical vapour deposition – From single- to triple-fused, *Eur. J. Org. Chem.*, 2019 (13), 2368–2375.

[16] Bengasi, G., Desport, J.S., Baba, K., Cosas Fernandes, J.P., De Castro, O., Heinze, K., and

Boscher, N.D., 2020, Molecular flattening effect to enhance the conductivity of fused porphyrin tape thin films, *RSC Adv.*, 10 (12), 7048–7057.

[17] Algethami, N., Sadeghi, H., Sangtarash, S., and Lambert, C.J., 2018, The conductance of porphyrin-based molecular nanowires increases with length, *Nano Lett.*, 18 (7), 4482–4486.

[18] Bodedla, G.B., Wang, H., Chang, S., Chen, S., Chen, T., Zhao, J., Wong, W.K., and Zhu, X., 2018, β-Functionalized imidazole-fused porphyrin-donor-based dyes: Effect of π-linker and acceptor on optoelectronic and photovoltaic properties, *ChemistrySelect*, 3 (9), 2558–2564.

[19] Tsuda, A., Furuta, H., and Osuka, A., 2000, Completely fused diporphyrins and triporphyrin, *Angew. Chem. Int. Ed.*, 39 (14), 2549–2552.

[20] Ryan, A.A., and Senge, M.O., 2013, Synthesis and functionalization of triply fused porphyrin dimers, *Eur. J. Org. Chem.*, 2013 (18), 3700–3711.

[21] Fukui, N., Yorimitsu, H., and Osuka, A., 2016, *meso-meso*-Linked diarylamine-fused porphyrin dimers, *Chem. Eur. J.*, 22 (51), 18476–18483.

[22] Ryan, A., Tuffy, B., Horn, S., Blau, W.J., and Senge, M.O., 2011, Carbazole-linked porphyrin dimers for organic light emitting diodes: Synthesis and initial photophysical studies, *Tetrahedron*, 67, 8248–8254.

[23] Feng, C.M., Zhu, Y.Z., Zhang, S.C., Zang, Y., and Zheng, J.Y., 2015, Synthesis of directly fused porphyrin dimers through Fe(OTf)$_3$-mediated oxidative coupling, *Org. Biomol. Chem.*, 13 (9), 2566–2569.

[24] Lee, S., Yamashita, K., Sakata, N., Hirao, Y., Ogawa, K., and Ogawa, T., 2019, Stable singlet biradicals of rare-earth-fused diporphyrin-triple-decker complexes with low energy gaps and multi-redox states, *Chem. Eur. J.*, 25 (13), 3240–3243.

[25] Lee, C.H., and Lindsey, J.S., 1994, One-flask synthesis of meso-substituted dipyrromethanes and their application in the synthesis of trans-substituted porphyrin building blocks, *Tetrahedron*, 50 (39), 11427–11440.

[26] Baldwin, J.E., Crossley, M.J., Klose, T., O'Rear, E.A., and Peters, M.K., 1982, Syntheses and oxygenation of iron(II) "strapped" porphyrin complexes, *Tetrahedron*, 38 (1), 27–39.

[27] Maciá, M.D., Campiña, J.M., Herrero, E., and Feliu, J.M., 2004, On the kinetics of oxygen reduction on platinum stepped surfaces in acidic media, *J. Electroanal. Chem.*, 564, 141–150.

[28] Xue, W., Zhou, Q., and Li, F., 2020, The feasibility of typical metal–organic framework derived Fe, Co, N co-doped carbon as a robust electrocatalyst for oxygen reduction reaction in microbial fuel cell, *Electrochim. Acta*, 355, 136775.